

MECHANISMS OF PARTICLE DISPERSION AND DEPOSITION IN A TURBULENT SQUARE DUCT FLOW

Jun Yao and Michael Fairweather

Institute of Particle Science and Engineering
School of Process, Environmental and Materials Engineering
University of Leeds
Leeds LS2 9JT, UK
m.fairweather@leeds.ac.uk

ABSTRACT

Particle dispersion in a square duct flow is studied using large eddy simulation combined with Lagrangian particle tracking under conditions of one-way coupling. The flow has a bulk $Re = 250k$, with six particle sizes ranging from 5 to $1000 \mu m$ examined. For the particles, predictions demonstrate that secondary flows within the duct dominate small particle dispersion, and result in a uniform distribution, whilst gravity promotes the deposition of large particles on the duct floor. A detailed analysis of the influence of the flow on particle distribution is provided through consideration of the particle dispersion function.

INTRODUCTION

Understanding the mechanisms of particle dispersion in turbulent flows is important in many industrial, environmental and energy-related processes. For example, the management of dust in clean rooms, chemical reactions involving a particulate catalyst, the flow of liquid and gas mixtures through process equipment, and the combustion of liquid sprays. Of particular interest in the present work is the processing and transportation of nuclear waste, much of which is stored as a liquid-solid sludge, and its behaviour in terms of the settling or non-settling characteristics of particles, their propensity to form solid beds, and the re-suspension characteristics of particles from a bed. The formation of particle beds can result in blockages to pipes and equipment, and lead to difficulties in obtaining dispersed particle flows from storage equipment for subsequent processing. The pumping of waste along pipes or ducts also gives rise to highly complex flows, where secondary flows caused, for example, by pipe bends can induce particle deposition. An understanding of how these flows behave during transportation is of clear benefit to more cost effective process design, continued operation and accelerated waste clean-up.

A great deal of work has been carried out to understand the mechanisms of particle dispersion in a variety of flows, for example, the plane wake, mixing layers, jet flows, and flows around a bluff body. Tang et al. (1992) used experimental and numerical methods to study particle dispersion mechanisms in a plane wake and demonstrated the importance of large scale vortex structures in self-organizing dispersion processes. Ling et al. (1998) and Fan et al. (2001) used direct numerical simulation to examine the dispersion of particles in three-dimensional mixing layers which are dominated by large scale, two-dimensional turbulent structures. Yuu et al. (1978) investigated the

turbulent diffusion mechanism of particles in a round jet and concluded that particle inertia and large scale turbulent eddies play an important role in the transport of particles. More recently, these findings were confirmed by Fairweather and Hurn (2007) who developed an anisotropic model of turbulent flows containing dispersed solid particles which was applied to gas-solid jets. Morsi and Alexander (1972) examined a two-phase flow around a cylinder and found that the effect of the lift force is small when compared with that of the drag force. Yao et al. (2003) also used direct numerical simulation to study the same problem and found that the mechanism of particle dispersion in the flow mainly depends on the repulsion force associated with the vortex sheet regions between two adjacent vortex structures with opposite sign. However, for particle-laden flows in a straight duct (square or rectangular), little work has been performed, and there is limited understanding of the mechanisms of particle dispersion.

A number of studies have focussed on turbulent single-phase flows through square ducts, including experimental investigations (Brundrett and Baines, 1964; Launder and Ying, 1972; Gessner et al. 1979), direct numerical simulations (Gavrilakis, 1992) and large eddy simulations (Madabhushi and Vanka, 1991). All of these studies have demonstrated that turbulence-driven secondary motions that arise in duct flows act to transfer fluid momentum from the centre of the duct to its corners, thereby causing a bulging of the streamwise velocity contours towards the corners. They also established that the Reynolds normal and shear stresses contribute equally to the production of mean streamwise vorticity. Compared with single-phase flows, there exist few studies of particle-laden turbulent flows in a duct. To date, two groups have conducted simulations in this field. Winkler et al. (2004) applied large eddy simulation, coupled with Lagrangian particle tracking, to study the preferential concentration of heavy particles in a duct flow, with their work focusing on particles with a low response time ($St = 0.25\sim 8$). Sharma and Phares (2006) also used direct numerical simulation and Lagrangian particle tracking to study secondary flow effects on particle transport and deposition in a square duct flow. However, in the latter work, the effects of gravity were neglected despite the consideration of large heavy particle behaviour in such flows. Both groups also focused on low Reynolds number turbulent flows ($Re_\tau = 360$ and 300 , respectively, based on the mean friction velocity and the duct width). As a consequence, particle dispersion mechanisms in square duct flows, particularly at high Reynolds numbers, have not been fully elucidated.

The present work uses large eddy simulation coupled with a Lagrangian particle tracking technique to study heavy particle dispersion in a high Reynolds number flow ($Re_\tau = 10,550$) in a straight, square duct. A wide range of particle sizes ($St = 0.24-9661$) have been investigated, with the distribution of particle velocity and position in the duct cross-section simulated, and the contribution of the secondary flow and gravity force to particle dispersion analysed. Further, the particle dispersion function has been applied to describe dispersion in the duct flow. Particle segregation and concentration near the floor of the duct are found to depend on particle size, and the link to flow structure is investigated.

MATHEMATICAL MODEL

Flow Configuration

The flow is three-dimensional and described by a Cartesian co-ordinate system (x, y, z) in which the z axis is aligned with the streamwise flow direction, the x axis is in the direction normal to the floor of the duct, and the y axis is in the spanwise direction. The corresponding velocity components in the (x, y, z) directions are, respectively, (u, v, w) . In modelling this flow, the boundary conditions for the momentum equations were no-slip at the duct walls. To avoid having to specify inflow and outflow conditions at the open boundaries of the duct, it was assumed that the instantaneous flow field was periodic along the streamwise direction, with the pressure gradient that drives the flow adjusted dynamically to maintain a constant mass flux through the duct. The friction Reynolds number, $Re_\tau = hu_\tau/\nu$, for the simulations was 10,550, corresponding to a bulk Reynolds number $Re_b \approx 250,000$. The dimensions of the square duct were $h \times h \times 4\pi h$, which in terms of wall units gives $L_x^+ = L_y^+ = 10,550$ and $L_z^+ = 132,576$. The streamwise length is sufficiently long to accommodate the streamwise-elongated, near-wall structures present in wall-bounded shear flows, with such structures rarely expected to be longer than approximately 1,000 wall units (Robinson 1991). Based on the Cartesian grid employed, $66 \times 66 \times 130$, the grid resolution was $\Delta x^+ = y^+ = 6.39$ wall units in the wall-normal directions and $\Delta z^+ = 40.80$ in the streamwise direction. The dimensionless integration time step used was $\Delta t = 6.66 \times 10^{-5}$ or, equivalently, $\Delta t^+ = 7.03 \times 10^{-1}$.

Large Eddy Simulation

In large eddy simulation only the large energetic scales of motion are directly computed, whilst the small scales are modelled. Any function is decomposed using a localised filter function, such that filtered values only retain the variability of the original function over length scales comparable to or larger than that of the filter width. The present work used a top hat filter as this fits naturally into a finite-volume formulation. This decomposition is then applied to the Navier-Stokes equations, for an incompressible Newtonian fluid with constant properties, giving rise to terms which represents the effect of the sub-grid scale (SGS) motion on the resolved motion. The SGS stress model used was the dynamic model of Germano et al. (1986), implemented using the approximate localization

procedure of Piomelli and Liu (1995) together with the modification proposed by di Mare and Jones (1991). This model represents the SGS stress as the product of a SGS viscosity and the resolved part of the strain tensor, and is based on the possibility of allowing different values of the Smagorinsky constant at different filter levels. In this formulation the model parameter is numerically well behaved, and the method is well conditioned and avoids the irregular behaviour exhibited by some implementations of the dynamic model. Test-filtering was performed in all space directions, with no averaging of the computed model parameter field.

Computations were performed using the computer program BOFFIN (Jones, 1991). The code implements an implicit finite-volume incompressible flow solver using a co-located variable storage arrangement. Because of this arrangement, fourth-order pressure smoothing, based on the method proposed by Rhie and Chow (1983), is applied to prevent spurious oscillations in the pressure field. Time advancement is performed via an implicit Gear method for all transport terms, and the overall procedure is second-order accurate in both space and time. The time step is chosen by requiring that the maximum Courant number lies between 0.1 and 0.3, with this requirement enforced for reasons of accuracy (Choi and Moin, 1994). The code is parallel and uses the message passing interface MPI-1.2. Time-averaged flow field variables reported below were computed from running averages during the computations.

Further details of the mathematical model employed, and the numerical algorithm and its implementation, may be found elsewhere (di Mare and Jones, 2003; Jones, 1991).

Lagrangian Particle Tracking

From the fluid velocity field V , particle motion was modelled using a Lagrangian approach (Fan et al. 2002) in which the particles are followed along their trajectories through the unsteady, non-uniform flow field. To simplify the analysis, the following assumptions were made: the particle-laden flow is dilute; interactions between particles are negligible; the flow and particles are one-way coupled, i.e. the effect of particles on the fluid is neglected; all particles are rigid spheres with the same diameter and density; and particle-wall collisions are elastic. The Lagrangian motion of a rigid, spherical particle suspended in a flow is governed by a force balance equation:

$$\frac{dV_p}{dt} = \frac{3\rho}{4\rho_p} \frac{C_D}{d_p} (V - V_p)|V - V_p| + \left(1 - \frac{\rho}{\rho_p}\right)g,$$

where V_p is the particle velocity, ρ_p particle density, d_p particle diameter, ρ fluid density and g gravity. C_D is the Stokes coefficient for drag, with $C_D = (1 + 0.15 Re_p^{0.687}) \cdot 24 / Re_p$, where Re_p is the particle Reynolds number, $Re_p = d_p |V - V_p| / \nu$. Even though a number

of possible forces can act on a particle, many of these may be neglected without any appreciable loss of accuracy, depending on the particle inertia. The most important force acting on the particle is the Stokes drag force, with gravity also important depending on the orientation of the flow. In this study, Stokes drag, gravity and buoyancy forces were considered, although the shear-induced Saffman lift force (Saffman, 1965) was neglected because it only assumes non-trivial magnitudes in the viscous sub-layer. Even in this region, however, it has been found to be an order of

magnitude smaller than the normal component of the Stokes drag force (McLaughlin, 1989). Due to particle-wall impaction, electrostatic charge can be generated at the particle surface and the duct wall (Yao et al. 2004). In this work, the straight square duct is set in the horizontal direction, such that the electrostatic force acting on a particle is much lower than the gravity effect by at least two orders of magnitude (Yao et al. 2006), and consequently can be neglected. Other forces acting on the particle, such as the hydrostatic force, Magnus effect, Basset history force and added mass force, were not taken into account due to their being orders of magnitude smaller than the three effects considered (Armenio and Fiorotto, 2001).

A fourth-order Runge-Kutta scheme was used to solve the equation of motion, given the initial particle location and velocity. The initial particle positions were distributed randomly throughout the duct, corresponding to an initially uniform wall-normal particle number density profile. The initial particle velocity was set equal to the fluid velocity, interpolated to the particle position. Particles were assumed to interact with turbulent eddies over a certain period of time, that being the lesser of the eddy lifetime and the transition time. For particles that moved out of the square duct in the streamwise direction, periodic boundary conditions were used to reintroduce them into the computational domain.

Particle and flow densities were set to $\rho_p = 2,500 \text{ kg m}^{-3}$ and $\rho = 1000 \text{ kg m}^{-3}$, respectively, with the kinematic viscosity of the flow $\nu = 1.004 \times 10^{-6} \text{ m}^2 \text{ s}^{-1}$. The particle relaxation time is $\tau_p = \rho_p d_p^2 / 18\rho\nu$, and the non-dimensional particle response time is defined as the particle Stokes number $St = \tau_p u_\tau^2 / \nu$, where the u_τ is the shear velocity (defined as $u_\tau = (\tau_w / \rho)^{1/2}$, with τ_w the wall shear stress). Six particle diameters were considered, namely $d_p = 5, 10, 50, 100, 500$ and $1000 \mu\text{m}$, with corresponding particle relaxation times, Stokes numbers and other relevant parameters given in Table 1.

Table 1 Parameters relevant to the simulations of particle dispersion and deposition.

$d_p / \mu\text{m}$	d_p^+	St	τ_p / s
5	1.32	0.24	3.46×10^{-6}
10	2.64	0.97	1.38×10^{-5}
50	13.19	24.15	3.46×10^{-4}
100	26.37	96.61	1.38×10^{-3}
500	131.87	2415.33	3.46×10^{-2}
1000	263.75	9661.31	1.38×10^{-1}

RESULTS AND DISCUSSION

Particle Simulations

Results obtained when particles are introduced to the flow are shown in Figure 1 which gives a perspective view of instantaneous distributions of particles crossing (x, y) planes at various downstream locations. For clarity of presentation, only a fraction of the dispersing particles is plotted. Small particles ($5 \mu\text{m}$, Figure 1 (a)) are seen to be fully distributed across all cross-sections. For medium size particles (50 and $100 \mu\text{m}$, Figures 1 (b) and (c)) the effect of

gravity leads to a progressive accumulation of particles within the lower half of the duct. At larger particle sizes ($500 \mu\text{m}$ and above, Figure 1 (d)), however, within a short time ($t^+ = 37,211$) the majority of particles are seen to deposit on the duct floor. In terms of the distribution of particles, the existence of competing gravitational and secondary flow influences clearly lead to different dispersion characteristics depending on particle size, with gravity decoupling particle behaviour from the effects of the secondary flow structure which subsequently affects the particle wall-normal distribution and deposition rate, particularly for larger particles.

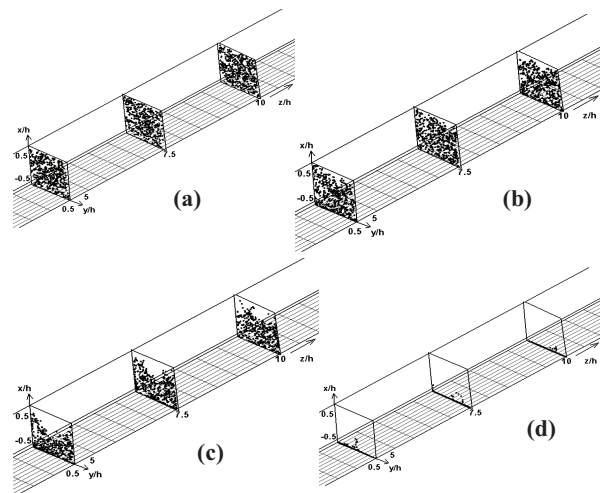


Figure 1. Instantaneous distribution of particles on (x, y) planes perpendicular to the streamwise direction: (a) $5 \mu\text{m}$ ($t^+ = 37,211$); (b) $50 \mu\text{m}$ ($t^+ = 153,494$); (c) $100 \mu\text{m}$ ($t^+ = 106,981$); (d) $500 \mu\text{m}$ ($t^+ = 37,211$).

Particle Dispersion Statistics

Figures 2 (a) to (c) show the relationship between the instantaneous particle location in the transverse direction, for three particle sizes, and the distribution of velocity in this direction at $t^+ = 13,954$. Location results are plotted in relation to the centre-line of the duct, with positive velocities indicating upward movement and negative downward movement. Small particles are well-dispersed, with gravity having little effect on their distribution, whilst particle velocities are distributed equally in both directions. Medium size particles ($100 \mu\text{m}$, Figure 2 (a)) are again well dispersed, although more of them (55%) tend to be associated with negative velocities acting in the same direction as gravity. For the largest particle sizes (500 and $1000 \mu\text{m}$, Figures 2 (b) and (c)) the majority of particles (84% and 89% respectively) are approaching the floor of the duct (at $x^+ = -5,275$), with their velocities also being mainly directed vertically downwards. Gravity therefore has a significant effect on the behaviour of these particles.

Figures 2 (d) to (f) again show the instantaneous distribution of particle position for the same particle sizes, but at the later time of $t^+ = 200,000$. Compared to the results of Figures 2 (a) to (c), the particles' velocity distribution is narrower and approximately symmetric about zero. In Figures 2 (b) and (c), more particles (75% and 68%

respectively) posses a velocity that is directed towards the duct floor, whilst at the later time (Figures 2 (e) and (f)) the particle velocity distribution is more symmetrical about $u_p^+ = 0$ with 39% and 42%, respectively, having negative velocities. Physically, at the later time, the particle velocity is much smaller than earlier in the simulations, with the particles being in closer proximity to the floor of the duct. For particles larger than $100 \mu m$, therefore, by $t^+ = 200,000$ gravity has caused them to approach and impact on the floor of the duct and to rebound off the wall with a velocity in the opposite direction. After rebounding, however, the particles cannot overcome the effects of gravity and again approach the duct floor. This process then repeats until the particles fully settle down on the lower surface of the duct.

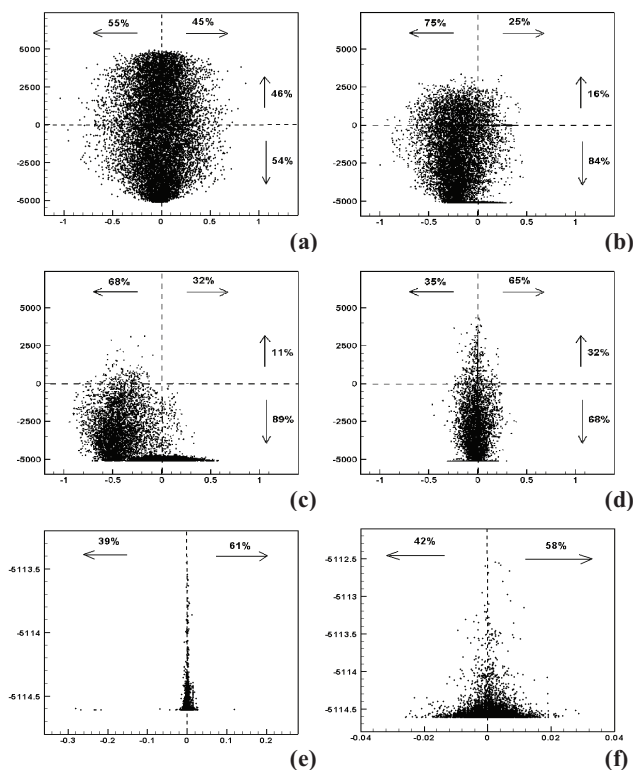


Figure 2. Instantaneous distribution of particle x^+ and u_p^+ : (a) $100 \mu m$; (b) $500 \mu m$; (c) $1000 \mu m$ ($t^+ = 13,954$); and (d) $100 \mu m$; (e) $500 \mu m$; (f) $1000 \mu m$ ($t^+ = 200,000$).

From the results of Figure 2, it is apparent that large (100 to $1000 \mu m$) particles approach the duct floor with time, whilst smaller (5 to $50 \mu m$) particles disperse well in the transverse direction, with that dispersion independent of time. Secondary flow effects may contribute in assisting the smaller particles to overcome the effects of gravity.

Turning to results for the spanwise direction, Figures 3 (a) to (c) show the instantaneous distribution of particle position and velocity in the horizontal direction, again at $t^+ = 13,954$, using the same approach as in the previous figure. As gravity has no effect in the direction considered, the influence of the secondary flow dominates particle location. All particle sizes are seen to be evenly dispersed along the spanwise direction, with particle velocities approximately symmetrical about $v^+ = 0$. Additionally, velocities in the

horizontal direction are of the same order of magnitude as those in the vertical direction (Figures 2 (a) to (f)).

Figures 3 (d) to (f) show the instantaneous distribution of the larger particles (100 to $1000 \mu m$) and their corresponding velocities in the spanwise direction at the later time of $t^+ = 200,000$. The particle velocity in the horizontal direction is again approximately symmetrical about $v^+ = 0$ although, compared to the results of Figures 3 (a) to (c), the particles' velocity distribution is narrower, particularly for the largest 500 and $1000 \mu m$ particles, as was also found for velocities in the transverse direction. This may contribute to the dominant influence of gravity with time on the motion of the largest particles. It may also be noted that for particles $\geq 100 \mu m$ the velocities in the spanwise direction (Figures 3 (d) to (f)) are larger than those in the transverse direction (Figures 2 (d) to (f)), with this trend becoming more significant with increasing particle size. This occurs because, at $t^+ = 200,000$, the large particles are in close proximity to the floor of the duct where transverse velocities are small but spanwise velocities

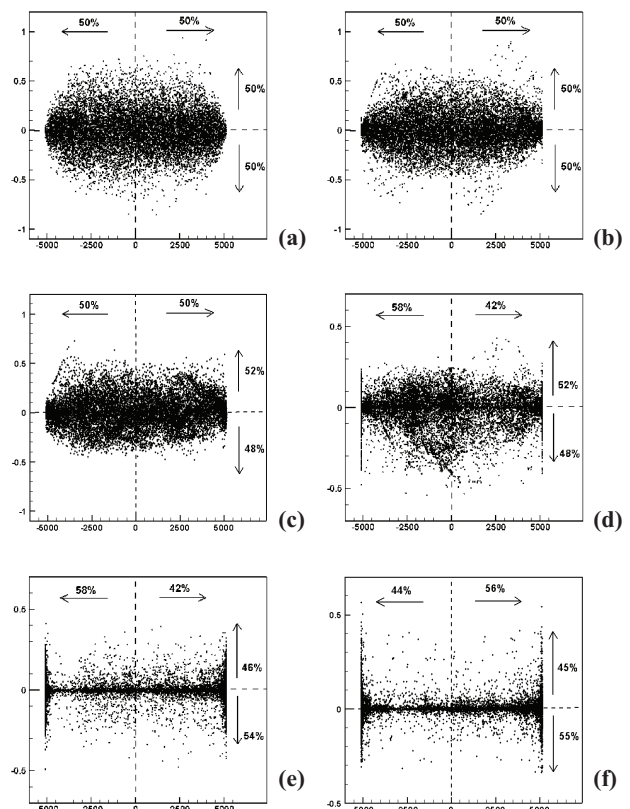


Figure 3. Instantaneous distribution of particle y^+ and v_p^+ : (a) $100 \mu m$; (b) $500 \mu m$; (c) $1000 \mu m$ ($t^+ = 13,954$); and (d) $100 \mu m$; (e) $500 \mu m$; (f) $1000 \mu m$ ($t^+ = 200,000$).

Particle Dispersion Function

To study particle dispersion in the duct flow quantitatively, the dispersion function in the transverse, x , direction for particles distributed in the duct can be introduced as:

$$D_{x(t)}^+ = \left(\frac{\sum_{i=1}^{n_t} (x_{i(t)}^+ - x_{m(t)}^+)^2}{n_t} \right)^{\frac{1}{2}}$$

where n_t is the total number of particles in the computational domain at time t , $x_{i(t)}^+$ is the particle displacement in the normal direction and $x_{m(t)}^+$ is the mean value, both relative to the centre-line of the duct. Similarly, the dispersion function in the spanwise direction can be obtained from:

$$D_{y(t)}^+ = \left(\frac{\sum_{i=1}^{n_t} (y_{i(t)}^+ - y_{m(t)}^+)^2}{n_t} \right)^{\frac{1}{2}}$$

where $y_{i(t)}^+$ is the particle displacement in the spanwise direction and $y_{m(t)}^+$ is the mean value, again relative to the centre-line.

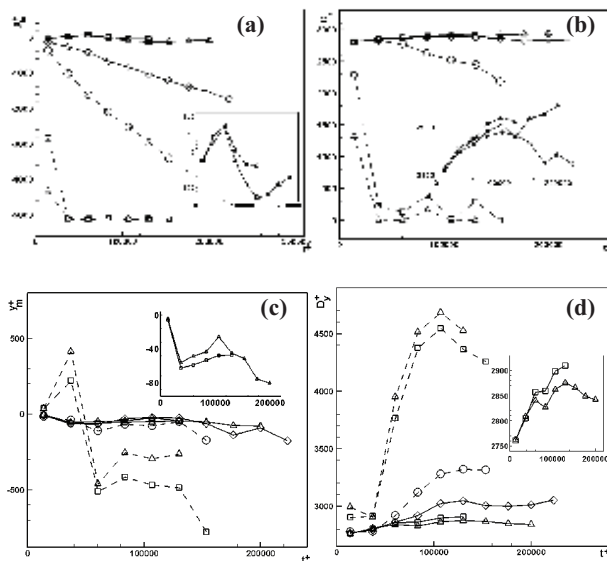


Figure 4. Particle dispersion with time: (a) mean displacement and (b) dispersion function in the transverse direction; (c) mean displacement and (d) dispersion function in the spanwise direction (\ominus - 5 μm ; \triangle - 10 μm ; \diamond - 50 μm ; \oplus - 100 μm ; \square - 500 μm ; Δ - 1000 μm).

Figures 4 (a) and (b) show results for the time-dependent particle dispersion in the transverse direction. In Figure 4 (a) the mean value of the particle displacement is seen to generally decrease with time due to gravity effects, with the rate of deposition increasing with particle size. For large particles (500 and 1000 μm) it only takes a short time ($t^+ = 37,211$) for them to approach the duct floor, whilst for medium sized particles (50 and 100 μm) the rate of deposition is slower and linear with time, with that rate increasing with particle size. For small particles (5 and 10 μm , also shown in detail in the inset of Figure 4 (a)), the mean value of the particle displacement in the transverse direction generally stays constant, although slightly oscillatory. The particle dispersion function (D_x^+) is presented in Figure 4 (b). It is clear from these results that for particles of 100 μm and larger the function decreases relatively rapidly with time, whilst for particles up to 50 μm in diameter the dispersion function remains approximately constant. Closer examination of results for the latter particles does, however, indicate that whilst the 5 and 10 μm particles disperse more in the transverse direction,

dispersion for the 50 μm particles increases with time until $t^+ = 106,981$, after which point it starts to decrease due to deposition. In close proximity to the duct floor, low-velocity streaks within the flow then cause the larger particles to segregate and concentrate, thereby further affecting particle dispersion. This phenomenon is analysed in the work (Fairweather and Yao, 2009).

Figures 4 (c) and (d) show equivalent results in the spanwise direction. Mean values of the particle displacement vary with time for all particle sizes, although the variation increases with size indicating that small particles tend to disperse well in the spanwise direction. For particles of 50 μm and larger, the mean value of particle displacement in the transverse direction (Figure 4 (a)) varies from $-5200 < x_m^+ < 100$ which compares to $-800 < y_m^+ < 450$ in the spanwise direction (Figure 4 (c)). This suggests that for these particles the effect of gravity is more significant than that of the secondary flow. However, for small particles (5 and 10 μm), the dispersion in both directions is approximately the same ($-140 < x_m^+ < 80$), indicating that gravity effects are unimportant for such particles. Figure 4 (d) shows the dispersion function where for particles of 50 μm and above values generally increase with time and particle size, whereas for 5 and 10 μm particles this function is approximately constant, and only increases slowly with time. This occurs since, under the influence of the secondary flows, larger particles tend to concentrate at the corners of the duct whilst small particles remain well dispersed (Fairweather and Yao, 2009).

CONCLUSIONS

In the square duct flow, competing gravitational and secondary flow effects dictate the dispersion and deposition of inertial particles. Gravity decouples particle behaviour from the secondary flow structure, thereby affecting the wall-normal distribution and deposition rate of large particles. The secondary flow dominates small particle behaviour, causing such particles to be well distributed throughout the flow. Gravity dominates large particle deposition in the transverse direction although, in the spanwise direction, it is the secondary flow that has a significant effect and causes particle concentration in the duct corners.

Analysis of the particle dispersion function shows that in the transverse direction small particles disperse more with time, whilst medium sized particles initially disperse until they start to approach to the duct floor when dispersion decreases. Large particles disperse less with time due to the effects of gravity. Comparing particle dispersion in the spanwise and transverse directions, the gravity effect is found to have a significant influence on the behaviour of large particles whilst having little effect on small particles.

ACKNOWLEDGEMENTS

This work was carried out as part of the TSEC programme KNOO and as such we are grateful to the EPSRC for funding under grant EP/C549465/1. The authors would also like to express their gratitude to Prof W.P. Jones for providing the BOFFIN LES code and for many helpful discussions on its use.

REFERENCES

- Armenio, V., and Fiorotto, V., 2001, "The Importance of the Forces Acting on Particles in Turbulent Flows", *Physics of Fluids*, Vol. 13, pp. 2437-2440.
- Brundrett, E., and Baines, W. D., 1964, "The Production and Diffusion of Vorticity in Duct Flow", *Journal of Fluid Mechanics*, Vol. 19, pp. 375-394.
- Choi, H., and Moin, P., 1994, "Effect of the Computational Time Step on Numerical Solutions of Turbulent Flow", *Journal of Computational Physics*, Vol. 113, pp. 1-4.
- Fairweather, M., and Hurn, J.-P., 2007, "Validation of an Anisotropic Model of Turbulent Flows Containing Dispersed Solid Particles Applied to Gas-Solid Jets", *Computer & Chemical Engineering*, Vol. 32, pp. 590-599.
- Fairweather, M., and Yao, J., 2009, "Mechanisms of Particle Dispersion in a Turbulent, Square Duct Flow", *AIChE Journal* (to appear).
- Fan, J. R., Yao, J., and Cen, K. F., 2002, "Antierosion in a 90° Bend by Particle Impaction", *AIChE Journal*, Vol. 48, pp. 401-412.
- Fan, J. R., Zheng, Y. Q., Yao, J., and Cen, K. F., 2001, "Direct Simulation of Particle Dispersion in a Three-Dimensional Temporal Mixing Layer", *Proceedings of The Royal Society of London Series A*, Vol. 457, pp. 2151-2166.
- Gavrilakis, S., 1992, "Numerical Simulation of Low-Reynolds-Number Flow Through a Straight Square Duct", *Journal of Fluid Mechanics*, Vol. 244, pp. 101-129.
- Germano, M., 1986, "A Proposal for Redefinition of the Turbulent Stresses in the Filtered Navier-Stokes Equations", *Physics of Fluids*, Vol. 19, pp. 2323-2324.
- Gessner, F. B., Po, J. K., and Emery, A. F., 1979, "Measurements of Developing Turbulent Flow in a Square Duct", In: Durst F., Launder B. E., Schmidt F. W., Whitelaw J. H., editors. *Turbulent Shear Flows 1*. New York: Springer-Verlag, pp. 119-136.
- Jones, W. P. BOFFIN, 1991, "A Computer Program for Flow and Combustion in Complex Geometries", Department of Mechanical Engineering, Imperial College of Science, Technology and Medicine.
- Launder, B. E., and Ying, W. M., 1972, "Secondary Flows in Ducts of Square Cross-Section", *Journal of Fluid Mechanics*, Vol. 54, pp. 289-295.
- Ling, W., Chung, J. N., Troutt, T. R., and Crowe, C. T., 1998, "Direct Numerical Simulation of a Three-Dimensional Temporal Mixing Layer with Particle Dispersion", *Journal of Fluid Mechanics*, Vol. 358, pp. 61-85.
- Madabhushi, R. K., and Vanka, S. P., 1991, "Large Eddy Simulation of Turbulence-Driven Secondary Flow in a Square Duct", *Physics of Fluids A*, Vol. 3, pp. 2734-2745.
- di Mare, L., and Jones, W. P., 2003, "LES of Turbulent Flow Past a Swept Fence", *International Journal of Heat Fluid Flow*, Vol. 24, pp. 606-615.
- Mclaughlin, J. B., 1989, "Aerosol Particle Deposition in Numerically Simulated Channel Flow", *Physics of Fluids*, Vol. 1, pp. 1211-1224.
- Morsi, S. A., and Alexander, A. J., 1972, "An Investigation of Particle Trajectories in Two-Phase Systems", *Journal of Fluid Mechanics*, Vol. 55, pp. 193-208.
- Piomelli, U., and Liu, J., 1995, "Large Eddy Simulation of Rotating Channel Flows Using a Localized Dynamic Model", *Physics of Fluids*, Vol. 7, pp. 839-848.
- Rhie, C. M., and Chow, W. L., 1983, "Numerical Study of the Turbulence Flow Past an Airfoil with Trailing Edge Separation", *ALAA Journal*, Vol. 21, pp. 525-532.
- Robinson, S. K., 1991, "Coherent Motions in the Turbulent Boundary Layer", *Annual Review of Fluid Mechanics*, Vol. 23, pp. 601-639.
- Saffman, P. G., 1965, "Lift on a Small Sphere in a Slow Shear Flow", *Journal of Fluid Mechanics*, Vol. 22, pp. 385-400.
- Sharma, G., and Phares, D. J., 2006, "Turbulent Transport of Particles in a Straight Square Duct", *International Journal of Multiphase Flow*, Vol. 32, pp. 823-837.
- Tang, L., Wen, F., Yang, Y., Crowe, C. T., Chung, J. N., and Troutt, T. R., 1992, "Self-Organizing Particle Dispersion Mechanism in a Plane Wake", *Physics of Fluids A*, Vol. 4, pp. 2244-2251.
- Winkler, C. M., Rani, S. L., and Vanka, S. P., 2004, "Preferential Concentration of Particles in a Fully Developed Turbulent Square Duct Flow", *International Journal of Multiphase Flow*, Vol. 30, pp. 27-50.
- Yao, J., Ji, F., Liu, L., Fan, J. R., and Cen, K. F., 2003, "Direct Numerical Simulation on the Particle Flow in the Wake of Circular Cylinder", *Progress in Natural Science*, Vol. 13, pp. 379-384.
- Yao, J., Zhang, Y., Wang, C. H., Matsusaka, S., and Masuda, H., 2004, "Electrostatics of the Granular Flow in a Pneumatic Conveying System", *Industrial & Engineering Chemistry Research*, Vol. 43, pp. 7181-7199.
- Yao, J., Zhang, Y., Wang, C. H., and Liang, Y. C., 2006, "On the Electrostatic Equilibrium of Granular Flow in Pneumatic Conveying Systems", *AIChE Journal*, Vol. 52, pp. 3775-3793.
- Yuu, S., Yasukouchi, N., Hirose, Y., Jotaki, T., 1978, "Particle Turbulent Diffusion in a Dust Laden Round Jet", *AIChE Journal*, Vol. 24, pp. 509-519.